Inorganic Materials, Vol. 39, No. 6, 2003, pp. 645–651. Translated from Neorganicheskie Materialy, Vol. 39, No. 6, 2003, pp. 761–768.

Fabrication and Properties of Semiconducting Barium Lead Titanate Ceramics Containing Low-Melting Glass Additions

O. Z. Yanchevskii, O. I. V'yunov, and A. G. Belous

Vernadsky Institute of General and Inorganic Chemistry, National Academy of Sciences of Ukraine, pr. Vernadskogo 32/34, Kiev, 03142

e-mail: belous@ionc.kar.net

Received April 26, 2002

Abstract—The structural parameters of yttrium-doped (Ba,Pb)TiO_3 solid solutions containing low-melting B_2O_3–PbO–SiO_2 (BPS) glass additions were determined by Rietveld powder-diffraction analysis. It is shown that the introduction of BPS enables dense, semiconducting ceramics containing up to 60 mol % $PbTiO_3$ to be produced by solid-state reactions followed by sintering at markedly reduced temperatures. Increasing the Pb content increases the lattice strain in the solid solutions, while BPS additions have the opposite effect. Sintering of BPS-containing materials leads to the formation of $(Ba_{1-\chi-y}Pb_\chi Y_y)(Ti_{1-\delta}Pb_\delta)O_3$ solid solutions on grain surfaces (core–shell structure).

INTRODUCTION

Rare-earth-doped barium lead titanate ceramics possess semiconducting properties and exhibit an anomalously large positive temperature coefficient of resistance (PTCR) near the Curie temperature t_C [1, 2]. In devising self-regulating PTCR ceramic heaters, an important point is control over the t_C of the ceramic, which determines the working temperature of the heater. It is well known that the t_C of $(1-\chi)BaTiO_3 - \chi PbTiO_3$ materials rises monotonically with $PbTiO_3$ content, from 120°C at $\chi = 0$ to 490°C at $\chi = 1$ [3]. At the same time, the high volatility of lead oxide impedes the fabrication of semiconducting ceramics exhibiting high-temperature PTCR behavior. For example, attempts to prepare dense $Ba_{1-\chi}Pb_\chi TiO_3$ materials with $\chi > 0.2$ ($t_C > 200$°C) by the conventional ceramic route were unsuccessful [4, 5]. This difficulty can be obviated by sintering green compacts in a lead-containing atmosphere or by reducing the sintering temperature. In the former case, use is made of hermetically sealed containers, and the green bodies are embedded in Pb-containing powder [6, 7], which markedly raises the production cost. Moreover, to obtain reproducible results, one must optimize the type and amount of Pb-containing powder, sintering temperature, and the type of the container, which adds complexity to the fabrication process [8].

A more promising approach is to reduce the sintering temperature of semiconducting barium lead titanate ceramics. This can be achieved by introducing additives that form an intergranular liquid phase during sintering [9–12]. Among the sintering additives ensuring good grain-boundary wetting, glass-formers are used most widely. In earlier studies, to improve the sintering behavior of ferroelectric ceramics, use was made of $BaO–B_2O_3–WO_3$ [12], $PbO–B_2O_3–Al_2O_3$ [13], $PbO–SiO_2$ [14], and $BaO–PbO–Bi_2O_3–TiO_2$ [15] glass-forming additives. However, knowledge of the effect of glass additions on the sintering behavior, structure, and semiconducting properties of barium lead titanate ceramics is still limited.

In this paper, we describe the sintering behavior and semiconducting properties of (Ba,Pb)TiO_3-based solid solutions prepared by solid-state reactions and containing low-melting B_2O_3–PbO–SiO_2 (BPS) glass-forming additives. The materials were doped with yttria, which is known to impart semiconducting properties to titanates in a broad concentration range and to ensure the high reproducibility of their transport properties [16]. The composition of the glass-forming additive was dictated by the following considerations: PbO is a binder preventing lead vaporization, while B_2O_3 and SiO_2 are typical glass-formers.

EXPERIMENTAL

To prepare BPS glass, an appropriate mixture of reagent-grade B_2O_3, PbO, and SiO_2 was melted in a platinum crucible at 800–1000°C, and the melt was poured into cold water. The resultant glass was crushed, ground, and sieved to obtain fine powder, which was then dried at 150°C.

Semiconducting (Ba,Pb)TiO_3-based solid solutions were prepared by solid-state reactions from appropriate mixtures of extrapure-grade $BaCO_3$, TiO_2, and Y_2O_3 and reagent-grade $PbTiO_3$. The mixtures were ground

0020-1685/03/3906-0645$25.00

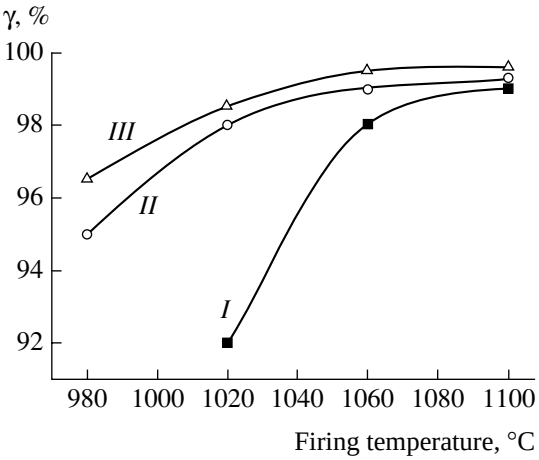

Fig. 1. Yield of solid solutions *I–III* as a function of firing temperature.

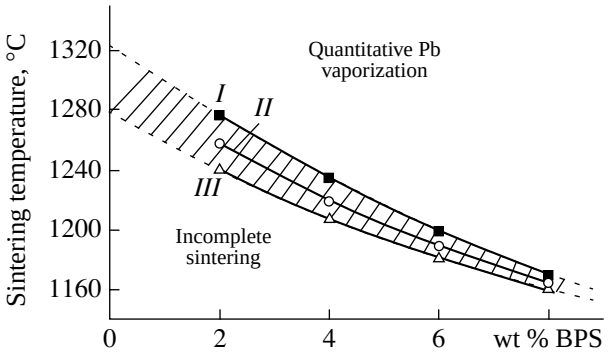

Fig. 2. Optimal sintering temperatures in systems *I–III*.

in bidistilled water for 6–10 h in a vibratory mill and, after drying, fired for 2 h at t_f = 900–1100°C. Next, the resultant material was mixed with 2–8 wt % BPS by vibration milling in bidistilled water for 6–8 h, and, after drying, an aqueous solution of poly(vinyl alcohol) was added as a binder. The mixture was pressed into disks 10 mm in diameter and ≃3 mm in thickness, which were sintered in the range t_{sint} = 1100–1300°C in air for 1 h at heating and cooling rates of 150–400°C/h.

The phase composition of the ceramics was determined by x-ray diffraction (XRD) analysis on a DRON-3M powder diffractometer (CuK_α radiation, 2θ = 10°–

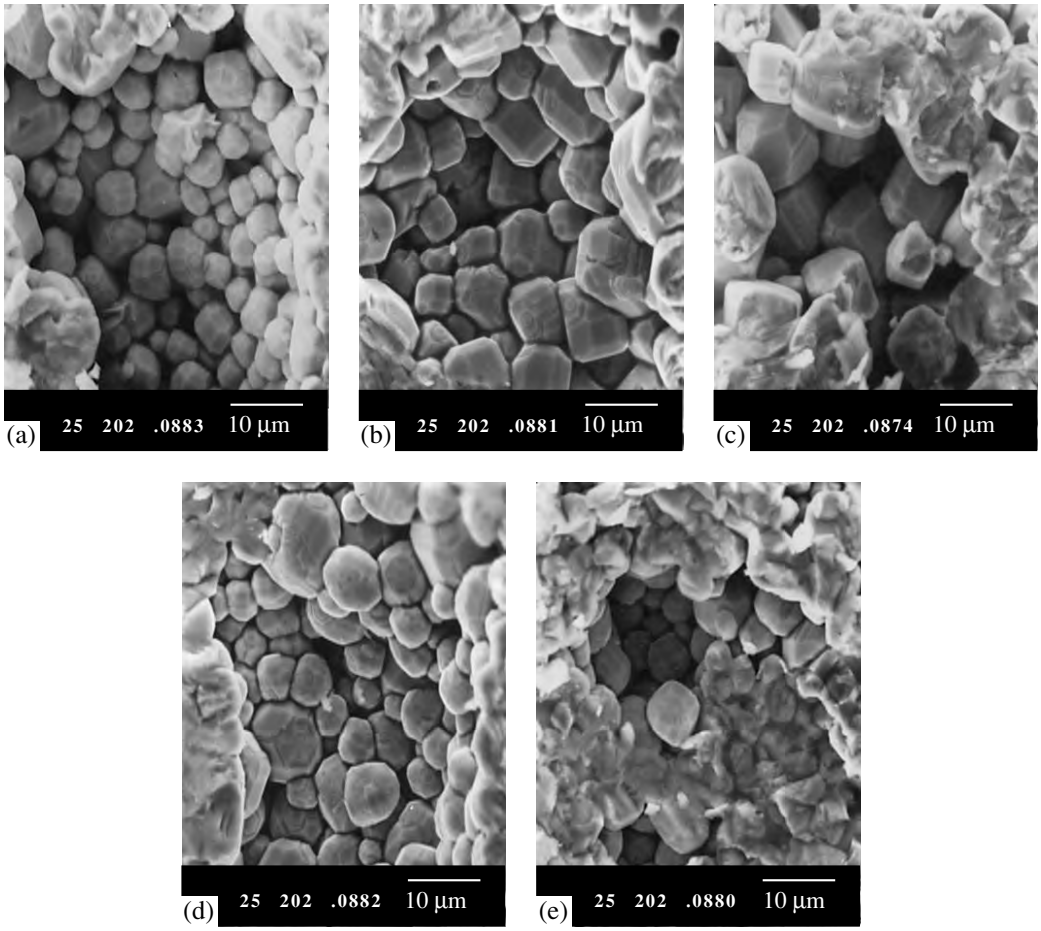

Fig. 3. SEM micrographs of ceramics obtained in systems (a, d, e) *I*, (b) *II*, and (c) *III*; (a–c) 8, (d) 4, (e) 6 wt % BPS.

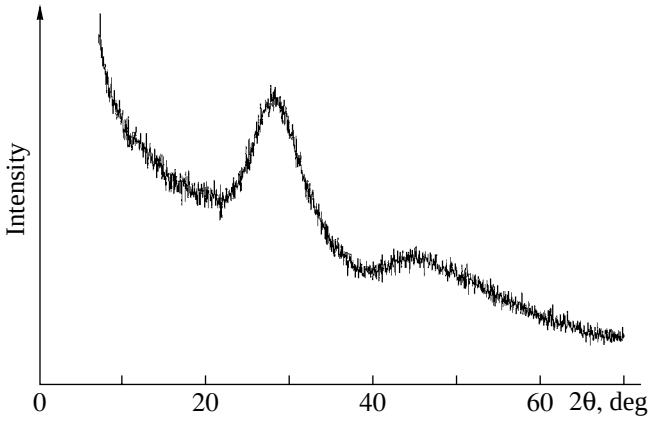

Fig. 4. XRD pattern of BPS.

150°, step-scan mode with a step size $\Delta(2\theta) = 0.02°$ and a counting time per data point of 10 s). As external standards, we used SiO_2 (2θ calibration) and Al_2O_3 (NIST SRM1976 intensity standard [17]). Structural parameters were refined by the Rietveld profile analysis method with the FullProf program (R_B and R_f no greater than 5%). Microstructures were examined by scanning electron microscopy (SEM) on a JEOL JCXA-733 SuperProbe. Ohmic contacts for electrical measurements were made by firing aluminum paste. The electrical resistivity of the semiconducting ceramics was measured during cooling from 560 to 20°C.

RESULTS AND DISCUSSION

To analyze the effect of BPS additions on the formation of semiconducting ceramics, we studied yttrium-doped titanate solid solutions differing in Pb content, with $t_C \simeq 250$ (system *I*), 280 (system *II*), and 320°C (system *III*). Data on the solid-solution yield (γ, %) indicate that, at a higher Pb content, (Ba,Pb)TiO_3-based solid solutions can be prepared at lower temperatures (Fig. 1). Above the optimal firing temperature, significant Pb losses occur. For this reason, we used firing temperatures at which the $BaCO_3$ content of the resulting materials did not exceed 2 wt %: t_f = 1060 (system *I*), 1020 (*II*), and 990°C (*III*).

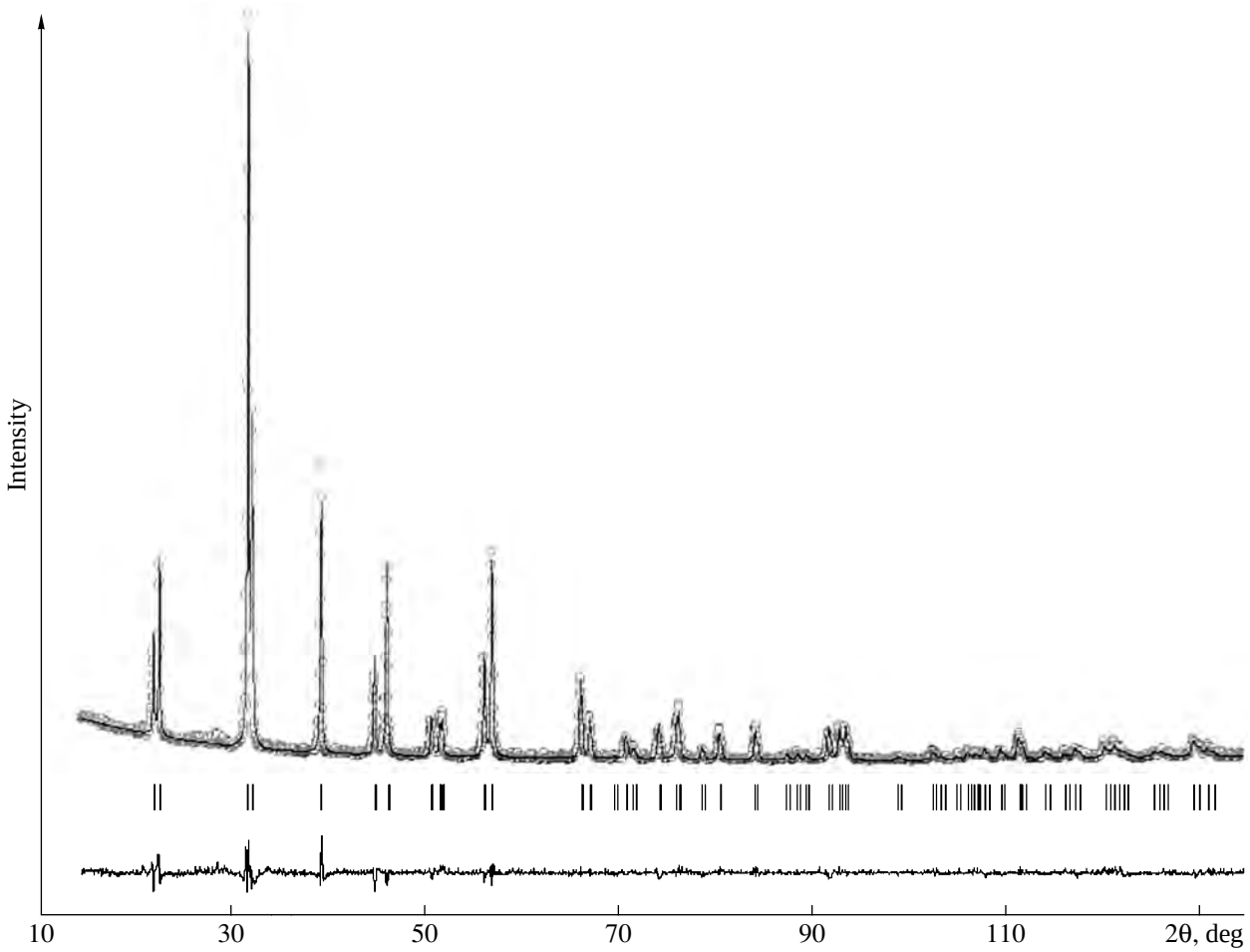

Fig. 5. Observed (open circles) and calculated (solid line) XRD patterns from a sample of system *I* (8 wt % BPS) and the difference plot. Vertical tick marks show peak positions.

Table 1. Structural parameters of Y-doped $Ba_{1-\chi}Pb_{\chi}TiO_3$ solid solutions containing 8 wt % BPS

System	*I*	*II*	*III*
$\chi_{nominal}$	0.35	0.45	0.55
a, Å	3.9574(1)	3.9491(1)	3.9392(1)
c, Å	4.0621(1)	4.0717(1)	4.0829(2)
c/*a*	1.0264	1.031	1.0365
V, Å^3	63.617(3)	63.498(3)	63.356(4)
χ_{meas}	0.299(6)	0.402(7)	0.498(7)
$\Delta\chi = \chi_{nominal} - \chi_{meas}$	0.051	0.048	0.052
$\Delta\chi/\chi_{nominal}$, %	14.5	10.6	9.4
z (Ba, Pb, Y)	0.502(2)	0.515(5)	0.522(3)
z (Ti)	0	0	0
z (O(1))	0.450(9)	0.437(9)	0.436(7)
z (O(2))	0.051(9)	0.075(6)	0.093(5)
R_B, %	4.20	4.13	4.07
R_f, %	4.28	4.02	3.56

Table 2. Structural parameters of Y-doped $Ba_{1-\chi}Pb_{\chi}TiO_3$ solid solutions with $\chi_{nominal} = 0.35$ (system *I*) containing different amounts of BPS

wt % BPS	0	4	6	8
a, Å	3.9612(2)	3.9595(1)	3.9585(1)	3.9574(1)
c, Å	4.0556(2)	4.0596(2)	4.0616(2)	4.0621(1)
c/*a*	1.0238	1.0253	1.026	1.0264
V, Å	63.636(5)	63.646(4)	63.644(3)	63.617(3)
χ_{meas}	0.280(6)	0.295(7)	0.286(6)	0.299(6)
$\Delta\chi = \chi_{nominal} - \chi_{meas}$	0.07	0.055	0.064	0.051
$\Delta\chi/\chi_{nominal}$, %	20.1	15.7	18.2	14.5
z (Ba, Pb, Y)	0.507(7)	0.500(9)	0.502(8)	0.502(8)
z (Ti)	0	0	0	0
z (O(1))	0.450(9)	0.44(1)	0.45(1)	0.45(1)
z (O(2))	0.058(9)	0.050(9)	0.055(9)	0.051(9)
R_B, %	4.41	4.25	4.15	4.20
R_f, %	4.04	4.34	3.78	4.28

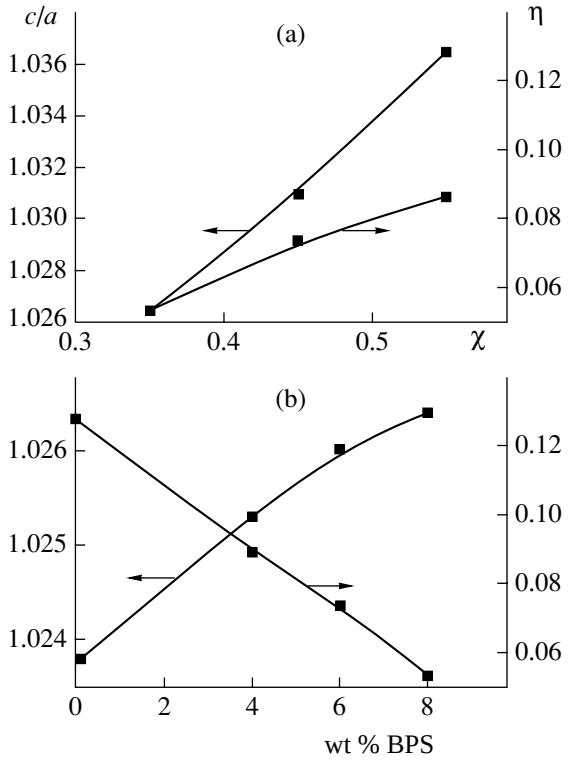

Fig. 6. Degree of tetragonality c/a and lattice strain η as functions of (a) Pb content (systems *I–III*, 8 wt % BPS) and (b) BPS content (system *I*).

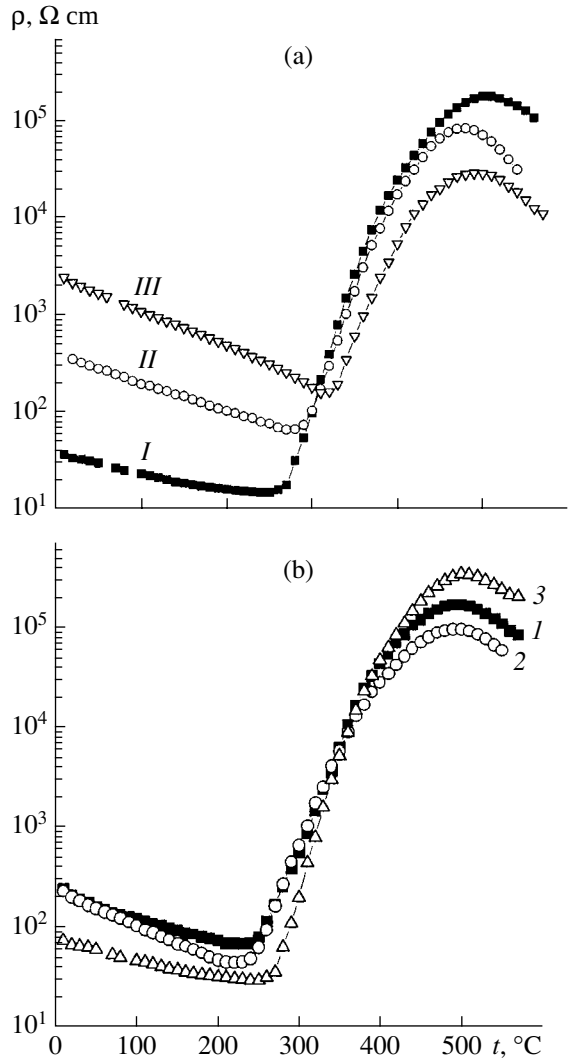

Fig. 7. Semilog plots of resistivity vs. temperature for (a) ceramics containing 8 wt % BPS (systems *I–III*) and (b) ceramics of system *I* containing (*1*) 4, (*2*) 6, and (*3*) 8 wt % BPS.

The introduction of BPS made it possible to markedly reduce (by 15–20°C/% BPS) the sintering temperature of the (Ba,Pb)TiO_3-based ceramics (Fig. 2), which can be understood in terms of liquid-phase sintering [18]. As can be seen in Fig. 2, t_{sint} decreases with increasing Pb content. At the same time, the difference in t_{sint} between systems *I–III* decreases with increasing BPS content. The grain size *D* of the ceramics depends more strongly on the Pb content than on the amount of the sintering additive (Fig. 3): *D* = 1.5–4 μm in system *I*, 2.5–5 μm in *II*, and 3.5–6 μm in *III*.

The XRD pattern of BPS shows two diffuse bands with *d* = 3.17 and 1.96 Å (Fig. 4), indicative of a short-range order. $Ba_{1-\chi}Pb_\chi TiO_3$ solid solutions have a tetragonal structure (sp. gr. *P*4*mm*), in which the degree of tetragonality (*c*/*a*) increases in going from $BaTiO_3$ to $PbTiO_3$ [3]. Figure 5 compares the observed and calculated XRD patterns from a sample in system *I*, and Table 1 lists the structural parameters of ceramics containing different amounts of Pb.

It can be seen from Table 1 and Fig. 6a that the degree of tetragonality in BPS-modified Y-doped $Ba_{1-\chi}Pb_\chi TiO_3$ increases with increasing χ. The structure of the solid solutions (sp. gr. *P*4*mm*) contains Ba, Pb, and Y in position 1*b* (1/2 1/2 *z*); Ti in position 1*a* (0 0 *z*); O(1) in position 1*a* (0 0 *z*); and O(2) in position 2*c* (1/2 0 *z*). The tetragonal distortion is due to the displacement of the Ba, Pb, Y, and O(2) ions in the +*z* direction (Table 1). As determined by Rietveld analysis, the occupancy of Pb^{2+} on the Ba site, χ_{meas}, is lower than $\chi_{nominal}$ by 9.5–15%, which is due to Pb vaporization.

Table 2 illustrates the effect of BPS additions on the structural parameters of the samples obtained in system *I*. With increasing BPS content, the *c*/*a* ratio increases (Fig. 6b), while the unit-cell volume varies very little. According to earlier studies [19], the reaction between PbO–B_2O_3 additions and $Ba_{1-\chi}Pb_\chi TiO_3$ leads to the formation of a core–shell structure, with a shell consisting of $BaTi(BO_3)_2$ or Pb-rich $Ba_{1-\chi}Pb_\chi TiO_3$, depending on the PbO : B_2O_3 ratio. Our XRD data for BPS-containing ceramics provide no evidence for borate formation. The observed variation of *c*/*a* with

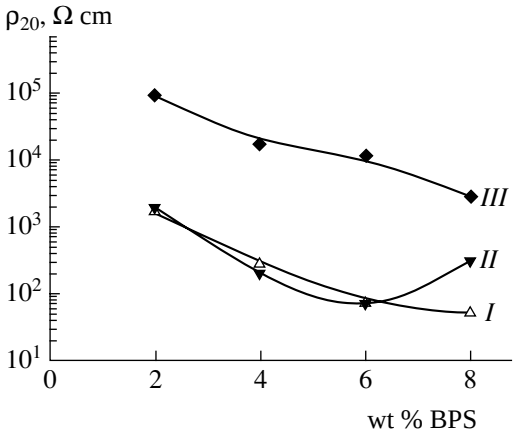

Fig. 8. Semilog plots of room-temperature resistivity vs. BPS content for ceramics of systems *I–III*.

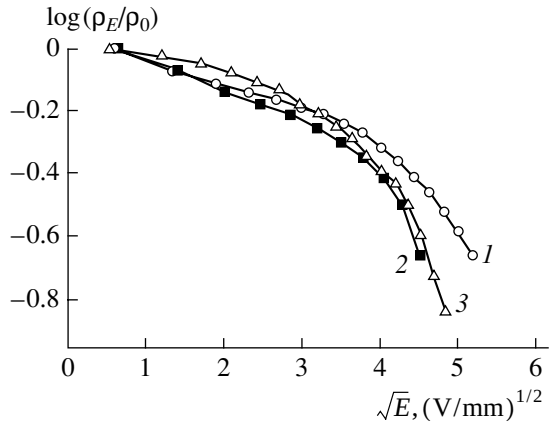

Fig. 9. Semilog plots of normalized resistivity versus the square root of the electric field for semiconducting ceramics of system *I* containing (*1*) 4, (*2*) 6, and (*3*) 8 wt % BPS.

BPS content (Fig. 6b) can be accounted for by an increase in the Pb content of the solid solution, which may be due to both the decrease in t_{sint} (and, hence, in Pb losses) and the incorporation of PbO from BPS into (Ba,Pb)TiO_3. However, an increase in χ must be accompanied not only by an increase in *c*/*a* but also by a reduction in unit-cell volume, which is at variance with the data in Table 2. As shown by Furaleva *et al.* [20], the $BaTiO_3$–PbO–BaO system contains $Ba(Ti_{1-x}Pb_x)O_3$ solid solutions, which are stable in an oxidizing atmosphere up to 1250°C and have a tetragonal structure. The unit-cell volume of these solid solutions increases linearly with *x*, in line with Vegard's law. Consequently, the reaction at the ceramic–glass interface may yield a multicomponent solid solution,

$$(1-\delta)(Ba_{1-\chi-y}Pb_{\chi-\delta}Y_y)TiO_3 + 2\delta PbO(glass) + \delta/2O_2 \longrightarrow (Ba_{1-\chi-y}Pb_\chi Y_y)(Ti_{1-\delta}Pb_\delta)O_3, \quad (1)$$

leading to the formation of a core–shell structure.

To assess the structural stability of BPS-modified (Ba,Pb)TiO_3, we evaluated lattice strain η from the slope of the plot of $\beta\cos\theta$ versus $\sin\theta$ [21], where $\beta\cos\theta = \lambda/D + 2\eta\sin\theta + \ldots$, β is the full width at half maximum of an XRD peak, λ is the x-ray wavelength, *D* is the grain size, and θ is the Bragg angle.

The results thus obtained demonstrate that increasing the Pb content of $Ba_{1-\chi}Pb_\chi TiO_3$ increases the lattice strain (Fig. 6a), while BPS additions stabilize the structure of the solid solution (Fig. 6b).

Figure 7a shows typical temperature dependences of resistivity for systems *I–III*. With increasing Pb content, t_C increases systematically, as does room-temperature resistivity, while the rise in resistivity around t_C becomes more gradual, indicating that the materials with $\chi > 0.6$ are unsuitable for PTC thermistors. The effect of BPS additions on the temperature-dependent resistivity of the ceramics obtained in system *I* is illustrated in Fig. 7b. With increasing BPS content, the onset of the rise in resistivity (t_C) shifts to higher temperatures, which can also be interpreted as evidence in favor of reaction (1), which increases the Pb content of the solid solution.

Figure 8 displays semilog plots of room-temperature resistivity ρ_{20} versus BPS content for ceramics of systems *I–III*. In going from system *I* to *III*, the optimal BPS content, ensuring a dense microstructure and low resistivity of the ceramics, increases from 4 to 8 wt %.

The magnitude of the varistor effect (electric-field-dependent resistivity) in PTCR ceramics is governed by the grain size, carrier concentration in the grain interior, and density of acceptor states. A sizeable varistor effect reduces the rise in resistivity near t_C, thereby limiting the application area of PTCR materials. Figure 9 shows semilog plots of normalized resistivity versus the square root of the electric field for the ceramics of system *I* containing 4–8 wt % BPS. It can be seen that there is no perfect correlation between the magnitude of the varistor effect and the BPS content. At the same time, increasing the amount of BPS and Pb content reduces the breakdown voltage, which is attributable primarily to an increase in average grain size.

CONCLUSIONS

The introduction of B_2O_3–PbO–SiO_2 glass-forming additions enables dense, semiconducting $Ba_{1-\chi}Pb_\chi TiO_3$ ceramics with $\chi \le 0.6$ to be produced by solid-state reactions followed by sintering at markedly reduced temperatures. The optimal BPS content is 4–8 wt %, depending on the Pb content. At a fixed percentage of BPS, increasing the Pb content increases the grain size and room-temperature resistivity of the ceramics, reduces the rise in resistivity near t_C, and increases the magnitude of the varistor effect. Moreover, with increasing Pb content, the lattice strain in the solid solutions increases, while BPS additions have the opposite effect.

Sintering of BPS-containing (Ba,Pb)TiO_3 materials leads to the formation of $(Ba_{1-\chi-y}Pb_\chi Y_y)(Ti_{1-\delta}Pb_\delta)O_3$ solid solutions on grain surfaces (core–shell structure).

REFERENCES

1. Sheftel', I.T., *Termorezistory* (Thermistors), Moscow: Nauka, 1973.
2. Gellerchik, B.A., Leikina, B.B., Sopina, V.N., *et al.*, *Vysokotemperaturnye pozistory—nagrevateli dlya bytovykh elektropriborov* (High-Temperature PTC Thermistors for Domestic Heaters), *II Vsesoyuznaya konferentsiya po aktual'nym problemam polucheniya i primeneniya segneto-, p'ezoelektricheskikh materialov* (II All-Union Conf. on the Critical Issues in the Fabrication and Application of Ferro- and Piezoelectric Materials), Moscow: NIITEKhIM, 1984, p. 240.
3. Venevtsev, Yu.N., Politova, E.D., and Ivanov, S.A., *Segneto- i antisegnetoelektriki semeistva titanata bariya* (Ferro- and Antiferroelectrics of the Barium Titanate Family), Moscow: Khimiya, 1985.
4. Leikina, B.B. and Kostikov, Yu.P., Choice of Dopants for the Preparation of Semiconducting (Ba,Pb,Ln)TiO_3 Solid Solutions, *Izv. Akad. Nauk SSSR, Neorg. Mater.*, 1989, vol. 25, no. 11, pp. 1933–1935.
5. Myasoedov, A.V. and Syrtsov, S.R., Positive Temperature Coefficient of Resistance in Pb-Doped Barium Titanate Ceramics, *Zh. Tekh. Fiz.*, 1997, vol. 67, no. 9, pp. 126–127.
6. Chun-Hung Lai and Tseung-Juen Tseng, Preparation and AC Electrical Response Analysis for (Ba,Pb)TiO_3 PTCR Ceramics, *J. Am. Ceram. Soc.*, 1993, vol. 76, no. 3, pp. 781–784.
7. Chun-Hung Lai, Yuh Yin Lu, and Tseung-Juen Tseng, Calculation and Modeling of Grain-Boundary Acceptor State for (Ba,Pb)TiO_3 Positive Temperature Coefficient Ceramics, *J. Appl. Phys.*, 1993, vol. 74, no. 5, pp. 3383–3388.
8. Kita Masakata and Onishi Kazuiti, Jpn. Patent Application no. 59-231935, 1984.
9. Belova, L.A., Gol'tsov, Yu.I., Prokopalo, O.I., and Raevskii, I.P., Preparation of Semiconducting $BaTiO_3$ Ceramics via Liquid-Phase Doping, *Izv. Akad. Nauk SSSR, Neorg. Mater.*, 1986, vol. 22, no. 6, pp. 1004–1008.
10. Freidenfel'd, E.Zh., Klyaine, R.Z., Bogomolov, A.A., *et al.*, Pyroelectric Properties of $PbTiO_3$-Based Ceramics with Glass Additions, *Izv. Akad. Nauk Latv. SSR, Ser. Khim.*, 1987, no. 6, pp. 655–657.
11. Howng, W.Y. and Cutchenon, C., Electrical Properties of Semiconducting $BaTiO_3$ by Liquid-Phase Sintering, *Am. Ceram. Soc. Bull.*, 1983, vol. 62, no. 2, p. 231.
12. Klyaine, R.Z. and Freidenfel'd, E.Zh., General Trends in the Modification of Ferroelectric Ceramics with Glass Additions, *Novye p'ezo- i sengetomaterialy i ikh primenenie* (New Piezo- and Ferroelectric Materials and Their Applications), Moscow: Moskovskii Dom Nauchno-Tekh. Propagandy, 1975, pp. 95–97.
13. Gol'tsov, Yu.I. and Shpak, L.A., Preparation and Properties of Semiconducting Barium Lead Titanate Ceramics, *Izv. Akad. Nauk SSSR, Neorg. Mater.*, 1990, vol. 26, no. 11, pp. 2418–2421.
14. Shittsa, D.A., Klimenko, L.I., and Freinfel'd, E.Zh., Effect of Oxide Additions on the Sintering Behavior and Properties of Lead Titanate Ceramics, *Neorg. Stekla, Pokrytiya Mater.*, 1985, no. 7, pp. 126–135.
15. Grossman, D.G. and Isard, J.O., Lead Titanate Glass-Ceramics, *J. Am. Ceram. Soc.*, 1969, vol. 52, no. 4, pp. 230–231.
16. Belous, A.G., V'yunov, O.I., Yanchevskii, O.Z., and Kovalenko, L.L., Thermodynamic and Experimental Investigation of the Effect of Rare-Earth Ions (Ln^{3+}) Nature on the Posistor Properties of $Ba_{1-x}Ln_x^{3+}TiO_3$, *Key Eng. Mater.*, 1997, vols. 132–136, part 1, pp. 1313–1316.
17. *Certificate of Analysis: Standard Reference Material 1976, Instrument Sensitivity Standard for X-ray Powder Diffraction*, Gaithersburg: National Inst. of Standards and Technology, 1991, pp. 1–4.
18. Milberg, Z.P., Klyaine, R.Z., Kutuzova, T.K., and Freidenfel'd, E.Zh., Structure, Properties, and Sintering Behavior of Modified Lead Titanate, *Izv. Akad. Nauk Latv. SSR, Ser. Khim.*, 1987, no. 5, pp. 542–546.
19. Hirata Akihino and Yamaguchi Takashi, Interfacial Reaction of $BaTiO_3$ Ceramics with $PbO–B_2O_3$-Glasses, *J. Am. Ceram. Soc.*, 1997, vol. 80, no. 1, pp. 79–84.
20. Furaleva, K.I., Prutchenko, S.G., and Politova, E.D., $Ba(Ti_{1-x}Pb_x)O_3$ Solid Solutions, *Neorg. Mater.*, 1998, vol. 34, no. 7, pp. 870–873 [*Inorg. Mater.* (Engl. Transl.), vol. 34, no. 7, pp. 725–728].
21. Ohsato, H., Imaeda, M., Takagi, Y., *et al.*, Microwave Quality Factor Improved by Ordering of Ba and Rare-Earth on the Tungsten Bronze-Type $Ba_{6-3x}R_{8+2x}Ti_{18}O_{54}$ (R = La, Nd, and Sm) Solid Solutions, *Proc. 11th IEEE Int. Symp. on Applications of Ferroelectrics*, Mountrex, 1998, pp. 509–512.